INVESTIGATION OF THE ELECTRON ENERGY SPECTRUM IN Bi-Sb *ALLOYS*

N. B. BRANDT, L. G. LYUBUTINA, and N. A. KRYUKOVA

Moscow State University

Submitted February 22, 1967

Zh. Eksp. Teor. Fiz. 53, 134–141 (July, 1967)

The de Haas–van Alphen effect in BiSb alloys containing from 1.7 to 4 at.% Sb is investigated at 1.6–4.2° K and field strengths varying between 1 and 12 kOe. The electron equal-energy surfaces decrease in volume with increasing Sb concentration, remaining similar to themselves with an accuracy to 8–10%. The decrease of the effective cyclotron masses with decrease of the corresponding extremal cross sections is satisfactorily described by the Cohen theory.[7] The best agreement between theory and experiment is obtained for an effective mass at the bottom of the conductivity band $m^*(0) = 0.002 \times 10^{27}$ g and an energy gap $E_g = 0.02$ eV between the conductivity band and valency band. The Fermi limiting energy and electron concentration are calculated for a nonquadratic dispersion law. The overlap is removed at ~5 at.% Sb.

INTRODUCTION

IT can by now be regarded as established that the electron dispersion in Bi is not quadratic. This is demonstrated first of all by the dependence of the electron effective mass on the Fermi energy,[1-4] and also by the unequal spacing of the Landau energy levels in strong magnetic fields.[5, 6] The dispersion of the electrons of Bi, with allowance for its deviation from parabolic, is usually described in terms of Cohen's theory.[7] However, the question of the accuracy with which this theory describes the energy spectrum of the electrons of Bi continues to remain unanswered, particularly owing to the lack of sufficient data[1, 2] on the change of the effective masses with decreasing Fermi energy, where this dependence should be particularly strong in accordance with Cohen's theory.

We investigate in this paper the energy spectrum of the electrons in which, as is well known,[8-12] the band overlap, together with the electron Fermi energy, decreases with increasing Sb concentration, making it possible to compare the experimental results with Cohen's theory and to obtain information regarding such important parameters of the spectrum as the value of the effective mass at the bottom of the band and the value of the energy gap between the conduction and valence bands.

MEASUREMENT PROCEDURE. SAMPLES

The anisotropy of the magnetic susceptibility $\Delta\chi \infty M/H^2$ of the samples was measured with a self-compensating magnetic torsion balance[13] in a homogeneous magnetic field from 1 to 12 kOe at temperatures 1.6–4.2° K.

The alloys for the samples were made of Bi (from GIREDMET [State Inst. for Rare Metals]) containing less than 1×10^{-4} of Pb, less than 1×10^{-5} of Ag, and less than 3×10^{-4} of Ni, and of Sb containing less than 2×10^{-5} of Cu, less than 4×10^{-4} Fe, and less than 5×10^{-5} As. Bi-Sb alloys of different concentrations were prepared by directly melting Bi with Sb in the required proportions. All the melts were thoroughly mixed in a sealed pyrex ampoule filled with helium gas, and kept in the molten state at 350–400° C for not less than 5–7 days, after which they were rapidly cooled.

Samples with up to 2 at.% Sb were grown at rates 0.4 cm/min by the Kapitza method.[14] To equalize the impurity concentration along the sample, recrystallization in the opposite direction was employed. However, at large Sb concentrations, metallographic investigations have revealed in samples grown at these rates a clearly pronounced substructure of cellular or dendrite type, due to the constitutional supercooling of the melt.[15] To reveal the substructure, we used both rough etching of the samples in nitric acid, as well as special fine etching, during the course of which the samples were first polished in a solution containing 6 parts of HNO_3 + 6 parts CH_3COOH and 1 part H_2O, then washed in HCl and water, dried in air, and etched in 1% solution of iodine in alcohol. The described fine etching was successfully used earlier to reveal the emergence of dislocations on the surface of Bi crystals.[16]

Table I. Characteristics of investigated samples*

Sample No.	c, at. % Sb	Mass, g	Growth conditions		Annealing conditions**	
			∇T, °C/cm	v, mm/hr	T, °C	t, days
1	0	0.084	17	270	without annealing	
2	1.7	0,248	17	270	170	7
3	2	0,194	17	270	266	12
4	2.4	0.299	17	30	without annealing	
5	2.5	0,185	17	270	266	44
6	2,9	0,464	17	1	170 266 266	7 5 30
7	3,1	0,250	30	1	without annealing	
8	3.4	0,185	90	1,5	without annealing	
9	3,6	0,420	30	1	266	45
10	4	0,166	90	1	without annealing	

*Samples for which a dendrite substructure was observed are not included in the table.

**All samples were investigated also before annealing. Sample No. 6 was annealed successively in three stages, and the measurements were made after each annealing stage.

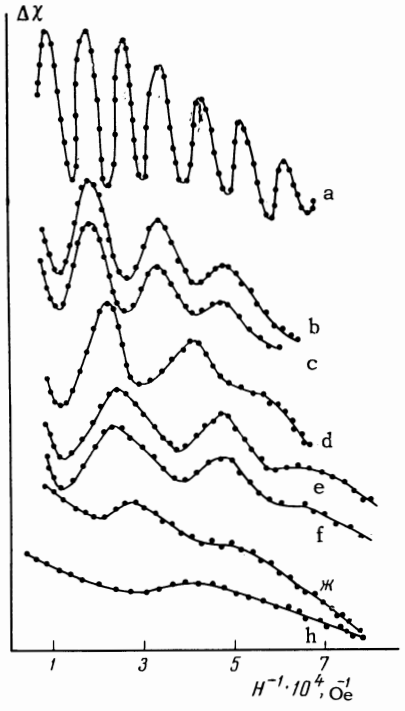

FIG. 1. Dependence of the anisotropy of the magnetic susceptibility $\Delta\chi \approx M/H^2$ for Bi-Sb alloys on the reciprocal field 1/H: a–initial Bi (sample No. 1, $\psi = 73°$, T = 1.6°K), b–sample No. 3 ($\psi = 127°$, T = 2.1°K), c–sample No. 3 ($\psi = 127°$, T = 4.2°K), d–sample No. 4 ($\psi = 80°$, T = 1.6°K), e–sample No. 6 ($\psi = 68°$, T = 2.1°K), f–sample No. 6 ($\psi = 68°$, T = 4.2°K), g–sample No. 9 ($\psi = 150°$, T = 1.6°K), h–sample No. 9 ($\psi = 80°$, T = 1.6°K). The scale along the y axis is the same only for curves b and c and d and e.

Samples containing more than 2 at.% Sb were grown slowly (up to 1 mm/hr) at large temperature gradients. With this, the rate of drawing and the temperature gradient were chosen in accordance with the data of [17], where growth under conditions in which there is no constitutional supercooling is considered in detail.

The crystallographic orientation of the samples was determined from the etch high spots with a goniometer, with accuracy ±0.5°, or from the lines on the cleavage plane, with accuracy 1–2°. Some of the samples were annealed under different conditions.

The data on all the investigated samples are listed in Table I (here c–calculated concentration,[1)] v–growth rate, and t–annealing duration).

MEASUREMENT RESULTS

Measurements of the anisotropy of the magnetic susceptibility $\Delta\chi$ were carried out with the magnetic field oriented in the trigonal-bisector plane. For each sample we plotted the dependence of the torque on the magnetic field intensity H at different orientations of the field relative to the trigonal axis of the sample (angle ψ). Characteristic plots of $\Delta\chi \propto M/H^2$ against 1/H for samples of the initial Bi and of Bi-Sb alloys are shown in Fig. 1.

To obtain the temperature dependence of the oscillation amplitude, the magnetic susceptibility was measured at two different temperatures (4.2 and 2.1° K) for angles ψ at which the oscillation amplitude was maximal. It should be noted that an analysis of the temperature dependence of the oscillations is greatly hindered when the Sb concentration is increased. This is connected, first, with the decrease in the oscillation amplitude and, second, with the decrease in the temperature dependence of the amplitude.

In measurements on samples with dendrite substructure, we observed oscillations whose frequency was close to the frequency of the oscillations of pure Bi for the corresponding angle ψ, these oscillations being most noticeable in strong fields. This served as an additional criterion for the sample quality.

Figure 2 shows the angular dependences of the oscillation frequencies for samples of the initial Bi (solid line) and Bi-Sb samples (the oscillation frequency $\Delta^{-1}(1/H)$ is connected with the extremal section S_m of the Fermi surface in a plane perpendicular to the H direction by $S_m = ehc^{-1}\Delta^{-1}(1/H)$[18]).

Figure 3 shows the dependence of the percentage change in the ratio S_m/S_m^{Bi}, averaged over the different angles ψ, on the calculated Sb concentration.

[1)]The chemical-analysis data obtained at GIREDMET for samples Nos. 3, 4, 5, 8, and 9 agree with the calculated concentration of Sb. within the accuracy limits (10 – 15%).

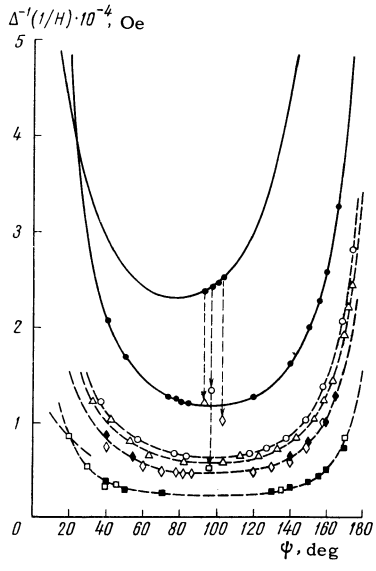

FIG. 2. Oscillation frequency $[\Delta(1/H)]^{-1} \infty S_m$ vs. the angle ψ: ● – initial Bi, ○ – sample No. 3, △ sample No. 5, ◊ – sample No. 6 before annealing, ♦ – the same after annealing, □ – sample No. 9 before annealing, ■ – the same after annealing. The dashed lines for the angular dependence of the frequencies are drawn for the alloys in analogy with the solid curve (the angular dependence for pure Bi) with suitable decrease of the ordinate scale.

The same figure shows data for the Bi-Sb alloys containing less than 1.6 at.% of Sb.[9]

An investigation of the influence of annealing at different rates (from 7 days at T = 150 – 170° C to 45 days at T = 266° C) has shown that the oscillation frequency does not depend on the annealing regime, whereas the oscillation amplitude increases somewhat after the annealing.

DISCUSSION OF RESULTS

1. Change in the shape of the electronic Fermi surface. Figure 4 shows the relative changes of the oscillation frequency (and consequently, of $\Delta S_m/S_m^{Bi}$) at different angles ψ. The angles ψ = 82–84° correspond to a change in the minimal section S_1 of the electronic ellipsoids. The change in the average section S_2 can be obtained by extrapolating the curves of Fig. 4 into the region of angles $\psi = 6°$. As seen from the figure, the decrease in the sections S_m of the electronic Fermi surface takes place, within the limits of the measurement accuracy (5–8%), at the same percentage ratio for all angles ψ. The angle of rotation of the ellipsoids can be assumed constant (accurate to ±2°). However, the lack of data on the changes in the section S_3 of the alloys under the influence of the Sb does not make it possible to state with assurance that the shape of the electronic Fermi surface does not change at all when its volume is decreased. Nonetheless, there are no grounds for assuming that this change is appreciable.

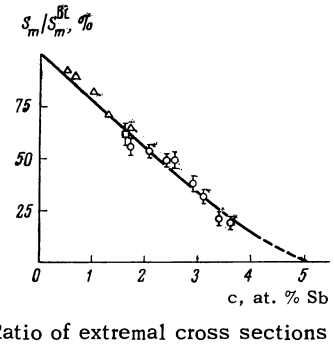

FIG. 3. Ratio of extremal cross sections of Bi-Sb alloys to the corresponding section for pure Bi vs. the calculated Sb concentration: ○ – present work, △ – [19], □ – [1].

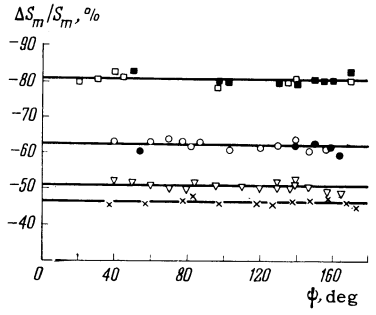

FIG. 4. Dependence of relative variation of the areas of the extremal sections of the electronic Fermi surface on the angle ψ: × – sample No. 3, ▽ – sample No. 4, ○ – sample No. 6 before annealing, ● – the same after annealing, □ – sample No. 9 before annealing, ■ – the same after annealing.

2. Electron dispersion in Bi-Sb alloys. According to Cohen's theory,[7] the electronic part of the Fermi surface of Bi is described by a formula that takes into account the deviation of the dispersion law from ellipsoidal and parabolic:

$$\frac{p_1^2}{2m_1}+\frac{p_2^2}{2m_2}+\frac{p_3^2}{2m_3}=E\left(1+\frac{E}{E_g}\right)-\frac{1}{E_g}\left(\frac{p_2^2}{2m_2}\right)^2, \quad (1)$$

where m_1, m_2, and m_3 are the effective masses at the bottom of the band. When the field H is oriented along the bisector axis, the non-ellipsoidal nature of the Fermi surface can be neglected, and the formulas for the extremal section S_1 and the effective mass m* take the form

$$S_1 = 2\pi m^*(0)E(1+E/E_g), \quad (2)$$

$$m^* = \frac{1}{2\pi}\frac{dS_m}{dE} = m^*(0)\left(1+\frac{2E}{E_g}\right), \quad (3)$$

where $m^*(0) = (m_1 m_3)^{1/3}$ is the cyclotron effective mass at the bottom of the band, E_g is the energy gap between the conduction band and the valence

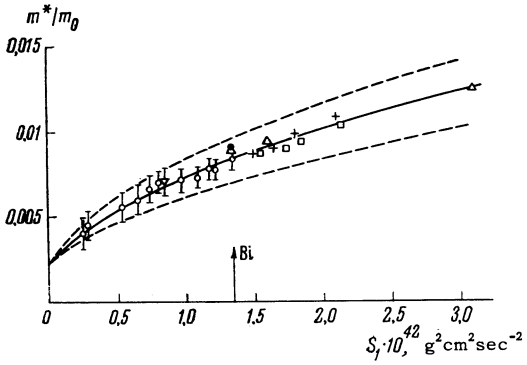

FIG. 5. Dependence of the ratio of the effective masses of the electrons in Bi-Sb alloys to the mass of the free electron on the minimum section S_1 of the Fermi surface: ● – data for pure Bi [21], □ – data of [3] for Bi-Te alloys, + – the same Bi-Se alloys, △ – data of [4] for Bi-Te alloys, ▽ – data of [1] for Bi + 1.6% Sb alloys. Solid curve – calculation in accord with Cohen's theory for $m^*(0) = 0.002 \times 10^{-27}$ g and $E_g = 0.02$ eV, dashed curves – for $E_g = 0.015$ eV (upper curve) and $E_g = 0.03$ eV (lower).

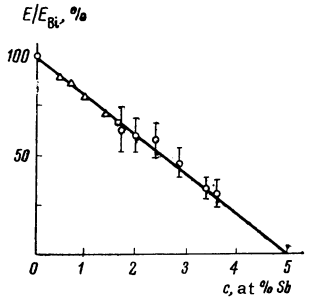

FIG. 6. Dependence of the ratio of the change of the electron Fermi energy in Bi-Sb alloys to the Fermi energy for pure Bi on the calculated Sb concentration: ○ – present work, △ – [9], □ – [1].

band, and E is the electron Fermi energy.

To determine the effective cyclotron masses in Bi-Sb alloys, we used data on the temperature dependence of the oscillation amplitudes ω_{T_1} and ω_{T_2} at temperatures $T_2 = 2T_1$, the ratio of the oscillation amplitudes is given by the formula[19]

$$\omega_{T_1} / \omega_{T_2} = \mathrm{ch}\,(2\pi^2 k T_1 / \beta H), \qquad (4)$$

which is valid in the region of helium temperatures in the case when the Dingle factor[20] is independent of the temperature (here $\beta = e\hbar/m^*c$ is double the effective Bohr magneton). For each angle ψ, the amplitudes of the oscillations were determined for different values of H, so that the quantity m*, calculated for each pair of curves, is an average for 20–30 measurements.

For comparison of the experimental data on m* with Cohen's theory, it is convenient to consider the dependence of the effective mass on the value of the corresponding cross section S_m for samples with different Sb contents. At $\psi = 80°$ this dependence can be described by the formula

$$m^*(S_1) = m^*(0)[1 + 2S_1/\pi m^*(0) E_g]^{1/2}. \qquad (5)$$

Figure 5 shows the dependence of m^*/m_0 on S_1 for Bi-Sb alloys (m_0—mass of the free electron). The same figure shows data for m^*/m_0 when S_1 increases, as obtained for Bi-Te and Bi-Se alloys,[3, 4] as well as the data of [1], in which cyclotron resonance and the Shubnikov–de Haas effect was investigated for a bismuth alloy with 1.6% Sb. The solid and dashed curves are drawn in accordance with formula (5) for different values of the parameters m*(0) and E_g. As seen from Fig. 5, the points agree experimentally quite well with the theoretical curve obtained for $m^*(0) = 0.002 \times 10^{-27}$ g and $E_g = 0.02$ V. However, the error in the determination of $m^*(S_1)$ is such that the values of E_g can vary within the range 0.013–0.03 eV (at $m^*(0) = 0.002$

Table II.

E, eV	E_g, eV	calculated in accord with (3)	Measurement method
0,0177	0,007	6	Galvanomagnetic measurements of Bi-Sb alloy [8]
0,025±0,005	0,015±0,002	4,3	Magnetooptic measurements [22]
0,022*	0,046*	2	de Haas-Van Alphen effect in Bi-Te alloy [4]
0,022[4]	0,024	2,8	Magneto-optical measurements [23]
0,027	0,014	4,85	Infrared reflection [24]
0,0276	0,015[22]	4,6	Shubnikov–de Haas oscillations in strong magnetic fields [6]
0,021±0,002	0,024±0,003	2,75	Galvanomagnetic and thermoelectric measurements of $Bi_{85}Sb_{15}$ alloy [25]
0,015	0,020	2,5	Tunneling [26]
0,031	0,013		Theory of Abrikosov and Fal'kovskii [27]
	0,02		Galvanomagnetic measurements [12]
0,027	0,02	3,7	Present work

*With allowance for errors, E = 0.021 – 0.024 and E_g = 0.035 – 0.070.

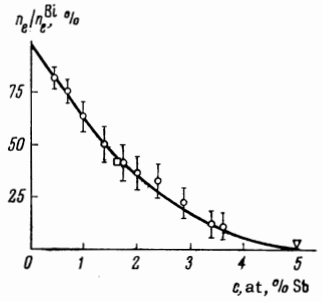

FIG. 7. Dependence of percentage ratio of number of electrons in Bi-Sb alloys to the number of electrons in the conduction band of pure Bi on the Sb concentration: O – our data, □ – [1], △ – [2]. The data for n_e/n_e^{Bi} at c < 1.6 at.% were obtained on the basis of the results of [9].

$\times 10^{-27}$ g) or 0.025–0.04 eV (at m*(0) = 0.003 $\times 10^{-27}$ g), and the effective mass at the bottom of the band can lie in the range (0.0035–0.0015) $\times 10^{-27}$ g.

For comparison, Table II lists data obtained by different workers for the parameters of the conduction band in Bi.

3. Change of the Fermi limiting energy for electrons in Bi-Sb alloys. To calculate the Fermi energy of the electrons in alloys with different Sb contents, we used Cohen's formula for a nonquadratic dispersion law:

$$\frac{S_m}{2\pi m^*} = \frac{E(1+E/E_g)}{1+2E/E_g}. \qquad (6)$$

The most probable values of the Fermi limiting energies E of the electrons in Bi-Sb alloys, calculated at E_g = 0.02 eV, are listed in Table III (the values of E for the case of quadratic dispersion and concentrations less than 1.7 at.% were taken from [9]).

Figure 6 shows the relative changes of the Fermi energy E/E_{Bi} in Bi-Sb alloys as functions of the concentration of Sb. We note that the values of E/E_{Bi} are not sensitive to variations of E_g in the range 0.015–0.04 eV.

4. Change in electron concentration. The number of electrons in the conduction band, n_e, can be estimated for Bi-Sb alloys by using the formula for a nonquadratic and nonellipsoidal dispersion law:

$$\frac{n_e}{n_e^{Bi}} = \left(\frac{E}{E_{Bi}}\right)^{3/2}\left(1+\frac{6E}{5E_g}\right)\Big/\left(1+\frac{6E_{Bi}}{5E_g}\right). \qquad (7)$$

Figure 7 shows the ratio of the number of electrons in Bi-Sb alloys to the number of electrons in Bi as a function of the Sb concentration. The calculations were carried out for E_g = 0.02 eV.

5. Change of band overlap in Bi-Sb alloys. To estimate the band overlap in Bi-Sb alloys it is necessary to know the change in the Fermi limiting energies for both the electrons and the holes. The values of the Fermi limiting energies for holes can be obtained by using the fact that the number of electrons n_e remains equal to the number of holes n_h when neutral Sb atoms are added to Bi.[9] Assuming that the dispersion of the holes is quadratic, we obtain for the ratio of the Fermi energies of the holes in the alloy and in pure Bi the formula

$$\frac{E_h}{E_h^{Bi}} = \left(\frac{n_h}{n_h^{Bi}}\right)^{2/3} = \left(\frac{n_e}{n_e^{Bi}}\right)^{2/3}. \qquad (8)$$

The band overlap in pure Bi is assumed to be

$$\varepsilon = E_h + E_e = 11{,}2 + 27{,}1 = 38{,}3 \text{ MeV}$$

The Fermi energy for holes E_h^{Bi} = 11.2 MeV was taken from [28]. The overlap decreases in proportion to the anitomony concentration in the alloys, reaching ϵ = 11.9 MeV for c = 3.6 at.% Sb. In accord with [12], the overlap is eliminated when c = 5 at.% Sb.

In conclusion, we take this opportunity to express sincere gratitude to A. I. Shal'nikov for interest in the work, and to thank V. N. Vigdorovich for supplying the high-purity bismuth and antimony.

[1] J. H. Kao, D. R. Brown, and R. L. Hartman, Phys. Rev. **136**, A858 (1964).

[2] G. E. Smith, Phys. Rev. Lett. **9**, 1187 (1962).

[3] N. B. Brandt and L. G. Lyubutina, Zh. Eksp. Teor. Fiz. **52**, 686 (1967) [Sov. Phys.-JETP **25**, 450 (1967)].

[4] D. Weiner, Phys. Rev. **125**, 1226 (1962).

[5] N. B. Brandt, E. A. Svistova, and G. Kh. Tabieva, ZhETF Pis. Red. **4**, 27 (1966) [JETP Lett. **4**, 17 (1966)].

Table III.

c, at % Sb	E, Mev		c, at % Sb	E, MeV	
	Quadratic dispersion law	Nonquadratic dispersion law		Quadratic dispersion law	Nonquadratic dispersion law
0	17,2±8%	27,1	2,0	11,5 ±15%	16,9
0.5	16,0 [9]	24,6	2,4	11,2 ±16%	16,3
1,0	14,4 [9]	21,9	2,9	9,35±15%	13,0
1,4	13,0 [9]	19,4	3,4	7,2±16%	9,4
1,7	12,1±13%	17,8	3,6	7,0±20%	9,2

[6] G. E. Smith, G. A. Baraff, and J. M. Rowell, Phys. Rev. **135**, A1118 (1964).
[7] M. H. Cohen, Phys. Rev. **121**, 387 (1961).
[8] A. L. Jain, Phys. Rev. **114**, 1518 (1959).
[9] N. B. Brandt and V. V. Shchekochikhina, Zh. Eksp. Teor. Fiz. **41**, 1412 (1961) [Sov. Phys.-JETP **14**, 1008 (1962)].
[10] S. Tanuma, J. Phys. Soc. Japan **14**, 1246 (1959); **16**, 2349 (1961); **16**, 2354 (1961)]
[11] G. A. Ivanov, Fiz. Tverd. Tela 5, 2409 (1963) [Sov. Phys.-Solid State 5, 1754 (1964)].
[12] N. B. Brandt and Ya. G. Ponomarev, Zh. Eksp. Teor. Fiz. **50**, 367 (1966) [Sov. Phys.-JETP **23**, 244 (1966)].
[13] N. B. Brandt and Ya. G. Ponomarev, PTÉ **6**, 114 (1961).
[14] P. L. Kapitza, Proc. Roy. Soc. **A119**, 358 (1928).
[15] C. Elbaum, Progr. Metal Phys. **8**, 203 (1959).
[16] L. C. Lovell and J. H. Wernick, J. Appl. Phys. **30**, 234 (1959).
[17] Dale M. Brown and F. K. Heuman, J. Appl. Phys. **35**, 1947 (1964).
[18] I. M. Lifshitz and A. M. Kosevich, Dokl. Akad. Nauk SSSR **96**, 963 (1954); Zh. Eksp. Teor. Fiz. **29**, 730 (1955) [Sov. Phys.-JETP **2**, 636 (1956)].
[19] J. S. Dillon and D. Shoenberg, Phil. Trans. Roy. Soc. (London), **A248**, 1 (1955).
[20] R. B. Dingle, Proc. Roy. Soc. **211**, 500 (1952); **212**, 38 (1952).
[21] M. S. Khaĭkin, R. T. Mina, and V. S. Édel'man, Zh. Eksp. Teor. Fiz. **43**, 2063 (1962) [Sov. Phys.-JETP **16**, 1459 (1963)].
[22] R. N. Brown, J. G. Mavroides, and B. Lax, Phys. Rev. **129**, 2055 (1963).
[23] W. E. Engeler, Phys. Rev. **129**, 1509 (1963).
[24] L. C. Hebel and P. A. Wolff, Phys. Rev. Lett. **11**, 368 (1963).
[25] D. M. Brown and S. J. Silverman, Phys. Rev. **136**, A290 (1964).
[26] L. Esaki and P. J. Stiles, Phys. Rev. Lett. **14**, 902 (1965).
[27] L. A. Fal'kovskiĭ and G. S. Razina, Zh. Eksp. Teor. Fiz. **49**, 265 (1965) [Sov. Phys.-JETP **22**, 187 (1966)].
[28] N. B. Brandt, T. F. Dolgolenko, and N. N. Stupochenko, Zh. Eksp. Teor. Fiz. **45**, 1319 (1963) [Sov. Phys.-JETP **18**, 908 (1964)].

Translated by J. G. Adashko
16